Chemistry & Biology
Review

GFP Family: Structural Insights into Spectral Tuning

Alexey A. Pakhomov[1] and Vladimir I. Martynov[1,*]
[1]Chromoproteins Chemistry Research Group, Shemyakin-Ovchinnikov Institute of Bioorganic Chemistry, Russian Academy of Sciences, 117997 Moscow, Russia
*Correspondence: vimart@list.ru
DOI 10.1016/j.chembiol.2008.07.009

Proteins homologous to green fluorescent protein (GFP) span most of the visible spectrum, offering indispensable tools for live cell imaging. Structural transformations, such as posttranslational autocatalytic and photo-induced modifications, chromophore isomerization, and rearrangements in its environment underlie the unique capacity of these proteins to tune their own optical characteristics. A better understanding of optical self-tuning mechanisms would assist in the engineering of more precisely adapted variants and in expanding the palette of GFP-like proteins to the near-infrared region. The latest advances in this field shed light upon multiple features of protein posttranslational chemistry, and establish some important basic principles about the interplay of structure and spectral properties in the GFP family.

Introduction

The GFP family consists of homologous proteins from marine organisms that contain chromophores derived from their internal amino acids. Most GFP-like proteins display bright fluorescence, with their optical properties encoded genetically and the chromophore center assembled posttranslationally by autocatalytic reactions inside the protein shell. Altogether, these features make it possible to fuse GFP-like fluorescent probes to virtually any desired target protein to monitor intracellular processes (Giepmans et al., 2006; Lukyanov et al., 2005; Shaner et al., 2007). Unlike low molecular weight fluorophores, the emission of GFP-like proteins is tuned by the surrounding protein matrix, enabling rational genetic manipulations to optimize protein optical properties. Consequently, photophysical properties of a fluorescent protein can be modified or improved by means of mutagenesis. The maturation, photochemistry, and photophysics of GFP-like proteins have been recently reviewed in detail (Remington, 2006).

Despite their pronounced spectral variability, coloration of GFP-like proteins is attained through a fairly conserved mechanism. Wild-type proteins of the GFP family have an 11-stranded β barrel structure (Figure 1A), with the conservative tyrosine and glycine residues in a chromogenic X-Tyr-Gly amino acid sequence. After polypeptide folding, the protein undergoes maturation via consecutive autocatalytic reactions within the chromogenic tripeptide. These reactions create a chromophore that includes a GFP-like structure, 4-(*p*-hydroxybenzylidene)-5-imidazolinone (*p*-HBI; Figure 1, structure **III**), as a primary building block. For the most part, spectral diversity stems from additional chemical modifications of the *p*-HBI core structure, and these autocatalytic reactions account for the coarse tuning of the protein to an appropriate spectral range. In this review, GFP-like proteins are classified into subfamilies according to chromophore structure and maturation mechanism. Further fine-tuning to a particular wavelength arises from different noncovalent interactions of the chromophore with its amino acid surroundings. Here we attempt to briefly summarize recent advances in our knowledge about structural tools in spectral tuning of GFP-like proteins.

GFP Subfamily

Wild-type and mutant proteins of the GFP subfamily emit light of blue, cyan, green, and yellow hues covering an emission range of approximately 440–527 nm (Heim et al., 1994; Ormo et al., 1996; Patterson et al., 2001). All naturally occurring proteins of this subfamily contain a *p*-HBI chromophore, which is generated by cyclization and oxidation reactions. The 11-stranded β barrel structure of GFP-like proteins contains an α helix running through the center of the barrel, which exhibits a dramatic bend located at the chromophore precursor XYG sequence. After protein folding into a β barrel structure, posttranslational chemistry comes into play. This self-modification process is apparently triggered by the bend in the central helix, which eliminates several main-chain hydrogen bonds and forces the Gly67 nitrogen into close proximity to the carbonyl carbon of Ser65 in preparation for the nucleophilic cyclization reaction (Figures 1A and 1B, structures **I** and **II**) (Barondeau et al., 2003). The cyclization reaction is obviously facilitated by the surrounding amino acid residues, which are arranged into a chromophore-forming pocket ensuring a scaffold for specific functional group catalysis. The highly conserved Arg96 and Glu222 residues (Figure 1A, magnification) have been proposed to be directly implicated in the catalysis of the chromophore cyclization-oxidation reactions (Wachter, 2007). Arg96 was proposed to play a primarily electrostatic role augmenting the nucleophilic strength of the Gly67 amide nitrogen (Wood et al., 2005). The carboxylate of Glu222 is likely to function as a general base, facilitating proton abstraction from the α-carbon of Tyr66 (Sniegowski et al., 2005) and together with Arg96 promoting α-enolate intermediate formation prior to oxidation reaction (Barondeau et al., 2006). The colorless GFP homolog from the hydromedusa *Aequorea coerulescens* (acGFPL) is an interesting exception, because wild-type acGFPL contains both the catalytic Arg96 and Glu222 residues, but is essentially nonfluorescent. The E222G substitution, which removes the evolutionarily invariant Glu222, results in the green fluorescent mutant of acGFPL (Gurskaya et al., 2003).

Although in all known natural GFP homologs, position 66 of the chromogenic tripeptide is occupied by a tyrosine, it appears that

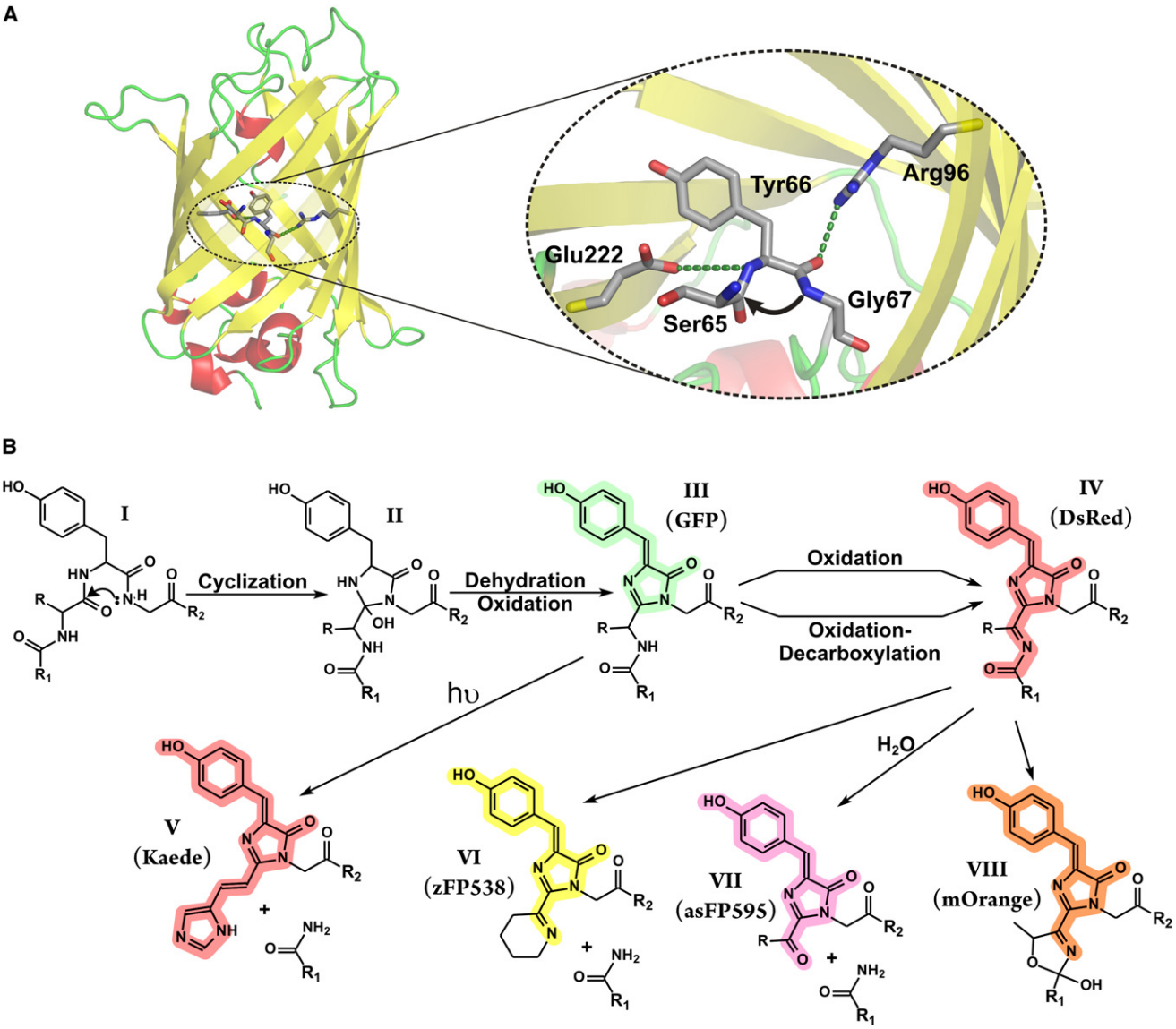

Figure 1. Posttranslational Reactions and Representative Chromophore Structures of GFP-like Proteins
(A) The β barrel structure of GFP-like proteins; precyclization state and catalytic Arg96 and Glu222 in the chromophore surroundings of avGFP (magnified).
(B) Chromophore biosynthesis and the diversity of chromophore chemical structures of GFP-like proteins (π-electron conjugation is indicated in color). The figure is not intended to show ionization states of the chromophore upon its biosynthesis.

Tyr66 is not essential for cyclization reaction. It can be substituted by phenylalanine, histidine, or tryptophan, producing GFP variants with a blue-shifted emission (Heim et al., 1994; Wachter et al., 1997). Although substitutions at position 66 do not influence backbone cyclization, they do affect posttranslational chemistry at later stages. The crystal structures suggest that Y66L substitution may either lead to the usual oxidative chemistry of the nonaromatic analog of a *p*-HBI chromophore, or yield an unusual crosslink between Leu66 and His148 (Rosenow et al., 2005). Likewise, high-resolution crystallography of the Y66F mutant of a GFP variant (GFPsol) showed a partition between native oxidation followed by Cα-Cβ double-bond formation and Cα-Cβ cleavage followed by a Y66F benzyl moiety loss. The obtained data suggest a common one-electron oxidized radical intermediate for chromophore biosynthesis in the GFP family (Barondeau et al., 2007). Together, these data also imply that Tyr66 controls proper oxidative chemistry in *p*-HBI chromophore biosynthesis.

The founding member of the family, avGFP (green fluorescent protein from *Aequorea victoria*), absorbs light at 395 nm, with a smaller peak at 475 nm, and emits green light at 508 nm. The predominant 395 nm absorbing form of the fluorophore is due to the uncharged phenol species, and the minor 475 nm form corresponds to the phenolate anion. The equilibrium between these states is controlled by the internal hydrogen bond network (Figure 2A) that promotes excited-state proton transfer (ESPT) from the phenol hydroxyl of the chromophore to the carboxylate group of Glu222. When excited, the neutral form, which would

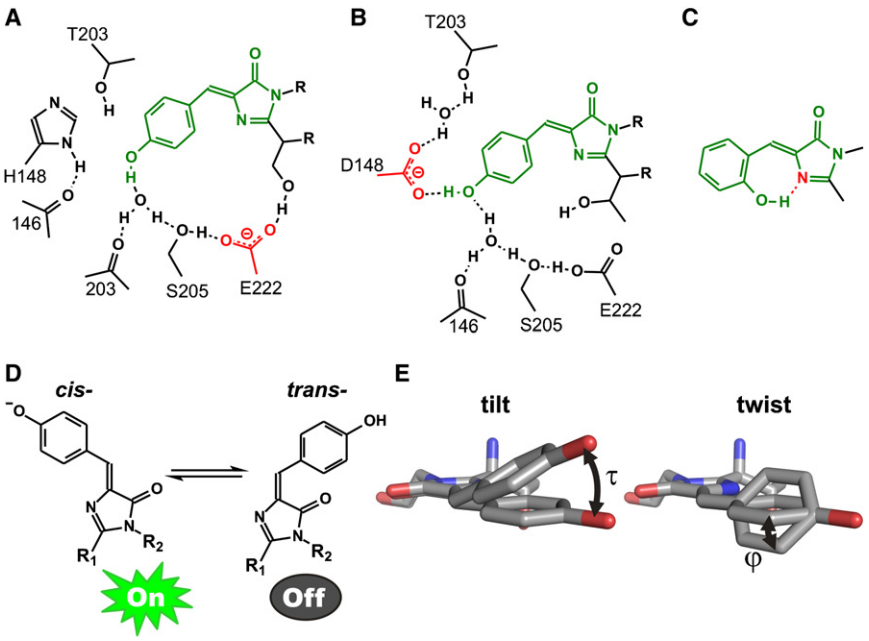

Figure 2. Chromophore Characteristics that Influence Spectral Properties of GFP-like Proteins

(A) Excited-state proton transfer in wild-type GFP. The chromophore is shown in green and the proton-accepting group is in red.

(B) Excited-state proton transfer in the S65T/H148D variant of GFP.

(C) Proposed excited-state proton transfer in the *ortho*-synthetic analog of a GFP chromophore.

(D) *cis-trans* isomerism of a *p*-HBI chromophore of Dronpa.

(E) Deviations from chromophore planarity: tilt and twist angles.

otherwise emit blue light, undergoes ESPT, generating a phenolate anion and emitting green light (Brejc et al., 1997; Palm et al., 1997). Reorientation or replacement of Glu222, as in the S65T and E222Q mutants, disrupts the ESPT pathway and leads to the loss of green emission after excitation of the neutral chromophore. However, the H148D substitution (Figure 2B) within the S65T variant restores green emission upon excitation of the neutral chromophore, suggesting that ESPT is switched on once again (Shu et al., 2007). In the avGFP mutant E222Q, the green fluorescence can also be recovered by the H148D substitution (Stoner-Ma et al., 2008). The chromophore hydroxyl is located in close proximity to Asp148, implying that the aspartate carboxylate is a proton acceptor in this case (Figure 2B) (Shi et al., 2007; Shu et al., 2007; Stoner-Ma et al., 2008). Spectroscopic and structural studies of asFP499, a protein from the sea anemone *Anemonia sulcata* var. *rufescens*, suggest that a short-distance ESPT mechanism may also be in operation in green-emitting anthozoan FPs. According to the X-ray structure and mutagenesis at position 158, ESPT between Asp158, Ser143, and the chromophore phenolic group is responsible for the presence of both neutral and anionic forms of the asFP499 chromophore over a wide pH range (Nienhaus et al., 2006).

Engineering variants with the ground-state equilibrium shifted toward the anionic form of the chromophore gave rise to so-called enhanced GFP (EGFP; emission at 510 nm) with a fluorescence 35 times brighter than that of wild-type GFP (Heim et al., 1995; Patterson et al., 1997). Mutations that shift the protonation equilibrium to the neutral phenol in the ground state and completely block ESPT were employed in the engineering of blue-emitting variants with a tyrosine-derived *p*-HBI chromophore (emission range 440–470 nm). With EGFP as a template an initial gene library was created, in which Thr65 was mutated to all amino acids and an additional three residues in close proximity to the chromophore (His148, Thr203, and Ser205) were simultaneously substituted by hydrophobic residues. Exhaustive screening of the initial library resulted in identification of the T65S/H148G/T203V/S205V variant of EGFP, which exhibited strong blue fluorescence and essentially no green emission. After additional several rounds of mutagenesis, a monomeric protein named mKalama1 with improved brightness was obtained (Ai et al., 2007). Another approach to engineering blue-shifted variants is to alter the chromophore π-electron structure by Y66H or Y66W substitutions, which produce derivatives with emission in the blue (blue fluorescent proteins; BFPs) and cyan (cyan fluorescent proteins; CFPs) region (Heim et al., 1994; Nguyen and Daugherty, 2005; Rizzo et al., 2004; Wachter et al., 1997). However, the consequence of such a dramatic change in the chromophore π-electron structure is poor fluorescence brightness and high propensity to photobleach, which are undesirable features for a genetic marker. In their approach, Mena et al. hypothesized that repacking the core of BFP could constrain motions of the chromophore that lead to reduced fluorescence brightness owing to internal conversion. Inspection of the crystal structure of BFP (Y66H/Y145F) revealed 12 positions in the chromophore vicinity to be mutated. As a result of these mutations, Azurite, a new BFP variant with improved brightness and photostability, has been isolated from a computationally designed library by flow cytometry (Mena et al., 2006).

Protonation/deprotonation equilibrium at the *p*-HBI chromophore was proposed to play a pivotal role in reversible photoswitching of Dronpa, a GFP homolog evolved from a *Pectiniidae* coral. Dronpa can be repeatedly and reversibly switched between a fluorescent on- and a nonfluorescent off-state by irradiation with light (Ando et al., 2004). The fluorescent and nonfluorescent forms were deduced to correspond to a deprotonated (anionic) and protonated (neutral) form of the chromophore, respectively (Habuchi et al., 2006). It has also been proposed that the back photoswitching mechanism involves efficient ESPT (Habuchi et al., 2005; Wilmann et al., 2006), which was supported by H/D exchange experiments (Fron et al., 2007). Recently, reversibly switchable Dronpa crystals have been obtained. The crystal structural data demonstrated that the primary event in the protein on-off switching is a light-activated *cis-trans* isomerization of the chromophore accompanied by complex structural rearrangements of nearby amino acid residues. Because of this intramolecular event the chromophore is exposed to different environments, which can influence its protonation

equilibrium. Thus, the resting fluorescent on-state of Dronpa is due to the *cis*-deprotonated (anionic) chromophore (Figure 2D), whereas the nonfluorescent off-state apparently corresponds to the protonated (neutral) *trans*-isomer (Andresen et al., 2007). Most recently, the photochromism of Dronpa has been studied by NMR in solution. On the basis of structural comparisons of the on- and off-states, Mizuno et al. proposed that in a fluorescent state the chromophore is tethered to the opposite β barrel by the hydrogen bond between the chromophore phenolate oxygen and the neighboring β barrel Ser142 hydroxyl group. This hydrogen bond apparently holds the two rings of the chromophore in a *cis*-configuration. The His193 imidazole ring, which is located below the chromophore phenyl moiety, stabilizes the entire chromophore planar conformation. This rigid structure favors the radiative relaxation process from the first electronic excited state to the ground state. By contrast, the *trans*-chromophore in the nonfluorescent state lacks both the hydrogen bond with Ser142 and chromophore stacking with His193. These structural changes increase the flexibility not only of the chromophore but also a part of the corresponding β barrel (Mizuno et al., 2008).

As a highly effective light emitter, GFP takes advantage of a chromophore that is fixed both covalently and via a hydrogen-bond network to neighboring amino acids. This intramolecular anchoring suppresses exocyclic torsional deformations which would otherwise lead to radiationless relaxation. Unlike fluorescent proteins, synthetic analogs of a GFP chromophore display much weaker fluorescence yields (Chen et al., 2007; Dong et al., 2007). In contrast to the natural *para*-isomer, an *ortho*-synthetic analog forms an intramolecular hydrogen bond between the phenolic OH group and the N(2) atom of the imidazolinone ring (Figure 2C), lowering the radiationless deactivation. The *ortho*-derivative, 4-(2-hydroxybenzylidene)-1,2-dimethyl-1H-imidazol-5(4H)-one, exhibited an absorption maximum at 385 nm and emission at 605 nm with an anomalously large Stokes shift and an increased fluorescence quantum yield, suggesting an efficient ESPT reaction. In contrast, an *o*-methoxy derivative, which does not display ESPT, showed an absorbance at ~370 nm and an emission with a normal Stokes shift at ~425 nm (Chen et al., 2007). To test the impact of chromophore rotation on a fluorescence quantum yield, Wu and Burgess prepared synthetic analogs of a GFP chromophore in which rotation about the bond connecting the two cycles was suppressed by complexation with a BF_2 entity. The fluorescence quantum yields of the conformationally locked boron-containing GFP analogs greatly increased, compared to the unconstrained noncomplexed molecules (0.86 and 0.0005, respectively) (Wu and Burgess, 2008).

To understand the structural basis for cyan emission, the X-ray structures of a cyan fluorescent protein amFP486 from *Anemonia majano* (λ_{em} = 486 nm) and its variants have been determined. amFP486 has a *p*-HBI chromophore that is chemically identical to that of avGFP. However, the fluorescence emission maximum of amFP486 is blue shifted by 23 nm relative to avGFP, owing to amino acid rearrangements in the chromophore-bearing pocket. Based on structural and spectroscopic studies, the fine-tuning of amFP486 fluorescence was proposed to be due to a quadrupole salt-bridge network (residues Arg72, Glu150, His199, and Glu217) responsible for maintaining the imidazole of His199 π-stacked against the chromophore's phenolic end. The placement of a positive charge on His199 near the phenolate moiety of the amFP486 chromophore was supposed to reduce the extent of charge delocalization, thus increasing the energy of the electronic transitions responsible for fluorescence (Henderson and Remington, 2005). Structural and mutagenesis studies of mTFP1, the monomeric version of *Clavularia* cyan fluorescent protein (λ_{em} = 492 nm), revealed an imidazole (His197) analogous to amFP486 His199 essential for cyan fluorescence (Ai et al., 2008). However, the crystal structure of dsFP483, a cyan-emitting protein from *Discosoma striata* (λ_{em} = 483 nm), demonstrated that this quadrupole salt-bridge network is not conserved, because in dsFP483 the amino acid position equivalent to His199 is occupied by a threonine. Moreover, in contrast to a proposed anionic chromophore of amFP486, Raman bands of wild-type dsFP483 appeared to be most similar to those of the neutral avGFP chromophore (Malo et al., 2008).

The longest-wavelength emission (527 nm) among the GFP-type chromophores is exhibited by yellow fluorescent protein (YFP), which is the result of the T203Y substitution (Ormo et al., 1996). The resulting π-π stacking between the Tyr203 and chromophore phenolic rings and an increased polarizability of π-stacked Tyr203 were assumed to be responsible for an additional tuning to longer excitation and emission wavelengths (Wachter et al., 1998). Recently, the red-emitting mutant of avGFP has been generated by directed evolution (Mishin et al., 2008). However, the red emission of this variant is proposed to be due to additional posttranslational modifications of the *p*-HBI chromophore, which are described below.

DsRed Subfamily

This subfamily includes orange, red, and far-red fluorescent proteins (emission range 550–650 nm) and chromoproteins (Figure 3). A number of genes encoding proteins of this subfamily have been recently cloned, either directly from marine organisms (Labas et al., 2002; Matz et al., 1999; Shagin et al., 2004; Karasawa et al., 2004), by directed evolution from monomeric DsRed (red fluorescent protein from *Discosoma* sp.) (Shaner et al., 2004), or via somatic hypermutation (Wang et al., 2004). To tune to the red spectral range, a *p*-HBI chromophore is further autocatalytically oxidized to form an acylimine substituent (Figure 1, structure **IV**) (Gross et al., 2000; Wall et al., 2000; Yarbrough et al., 2001). The oxidation mechanism and amino acids responsible for this reaction presently remain unidentified.

Structural studies suggest that DsRed has a tetrameric quaternary structure and, even after prolonged maturation, the DsRed tetramer contains green and red monomers in about a 1:1 ratio (Gross et al., 2000). Green-emitting anionic *p*-HBI has been postulated to be an intermediate in DsRed chromophore synthesis. However, it has recently been proposed that the "red" chromophore of DsRed and related chromoproteins is produced from a blue-emitting neutral form of a *p*-HBI chromophore, the green anionic species being a dead-end product (Verkhusha et al., 2004). Unlike the avGFP ground state, the phenolate oxygen of the mature DsRed-like chromophore appears to be permanently charged (Yarbrough et al., 2001).

Like in other organic molecules, the extent of a GFP-like protein spectral shift correlates with the degree of extension of a chromophore π-electron system and with the efficiency of π-orbital overlapping, which reflects the chromophore planarity. Polarity of the

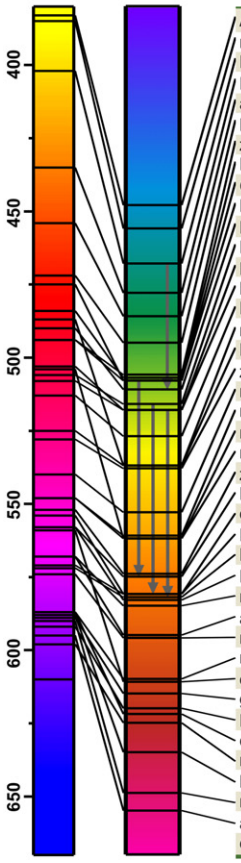

Protein	Absorbance maximum, nm	Fluorescence emission maximum, nm	Molar extinction coefficient, x10^3 M^{-1}cm^{-1}	QY[a]	Subfamily/ Chromophore	References[b]
Azurite	384	450	26.2	0.55	GFP-Y66H	Mena et al., 2006
mKalama1	385	456	36	0.45	GFP	Ai et al., 2007
PS-CFP (cyan)[c]	402	468	34	0.16		Chudakov et al., 2004; Lukyanov et al., 2005
ECFP	434	477	26	0.4	GFP-Y66W	Heim et al., 1994; Patterson et al., 2001
amFP486	454	486	ND[f]	0.71	GFP	Matz et al., 1999; Henderson and Remington, 2005
MiCy	472	495	27.25	0.9		Karasawa et al., 2004
zFP506	494	506	ND	ND	GFP	Matz et al., 1999; Pakhomov and Martynov, 2007
EGFP	484	507	53	0.6	GFP	Heim et al., 1995; Patterson et al., 1997
GFP	475; 395	508	25	0.79	GFP	Ormo et al., 1996; Patterson et al., 1997
DendFP (green)[c]	492	508	90	0.65	GFP	Pakhomov et al., 2004; Gurskaya et al., 2006
PS-CFP (green)[c]	490	511	27	0.19		Chudakov et al., 2004; Lukyanov et al., 2005
EosFP (green)[c]	506	516	72	0.70	GFP	Wiedenmann et al., 2004; Nienhaus et al., 2005
Dronpa	503	518	95	0.85	GFP	Ando et al., 2004; Andresen et al., 2007
Kaede (green)[c]	508	518	98.8	0.80	GFP	Ando et al., 2002; Mizuno et al., 2003
EYFP	514	527	84	0.61	GFP	Ormo et al., 1996; Wachter et al., 1998
mHoneydew[d]	487	537	17	0.12		Shaner et al., 2004
PhiYFP	525	537	115	0.60		Shagin et al., 2004
zFP538	528	538	ND	ND	DsRed-related	Matz et al., 1999; Remington et al., 2005
mBanana	540	553	6	0.70		Shaner et al., 2004
mKO	548	561	51.6	0.60		Karasawa et al., 2004
mHoneydew[d]	504	562	17	0.12		Shaner et al., 2004
mOrange	548	562	71	0.69	DsRed-related	Shaner et al., 2004; Shu et al., 2006
z2FP574	552	574	ND	ND	DsRed-related	Labas et al., 2002; Pakhomov and Martynov, 2007
DendFP (red)[c]	557	575	35	0.68	Kaede	Pakhomov et al., 2004; Gurskaya et al., 2006
dTomato	554	581	69	0.69		Shaner et al., 2004
EosFP (red)[c]	571	581	41	0.55	Kaede	Wiedenmann et al., 2004; Nienhaus et al., 2005
Kaede (red)[c]	572	582	60.4	0.33	Kaede	Ando et al., 2002; Mizuno et al., 2003
DsRed	558	583	75	0.79	DsRed	Matz et al.,1999; Gross et al.,2000; Shaner et al.,2004
mTangerine	568	585	38	0.30		Shaner et al., 2004
asFP595 (KFP)	568	595	56.2	<0.001	DsRed-related	Lukyanov et al., 2000; Tretyakova et al., 2007
mStrawberry	574	596	90	0.29	DsRed	Shaner et al., 2004; Shu et al., 2006
mCherry	587	610	72	0.22	DsRed	Shaner et al., 2004; Shu et al., 2006
eqFP611	559	611	78	0.45	DsRed	Wiedenmann et al., 2002; Petersen et al., 2003
gtCP[e]	589	615	ND	chromo	DsRed	Gurskaya et al., 2001; Martynov et al., 2003
Rtms5[e]	592	620	80	chromo	DsRed	Prescott et al., 2003
cgCP[e]	587	622	ND	chromo	DsRed	Gurskaya et al., 2001; Pakhomov et al., 2006
mRaspberry	598	625	86	0.15		Wang et al., 2004
Katushka	588	635	65	0.34		Shcherbo et al., 2007
mPlum	590	649	41	0.10		Wang et al., 2004
aeCP-AQ143	595	655	90	0.04		Shkrob et al., 2005
cjBlue	610	ND	66.7	chromo	DsRed	Chan et al., 2006

Figure 3. Spectral Characteristics and Chromophore Types of the Wild-Type and Mutant Proteins of the GFP Family
[a]Fluorescence quantum yield.
[b]References are given for protein quantitative spectral and chromophore structural data.
[c]For photoconvertible fluorescent proteins, transition from one emission maximum to another is shown by the arrow on the emission scale.
[d]mHoneydew has two absorbance and fluorescence emission maxima.
[e]Spectral characteristics are given for the fluorescent mutants of chromoproteins.
[f]Not determined.

surrounding amino acids also contributes to the position of the absorbance/fluorescence maximum. The DsRed chromophore adopts a planar conformation with the tyrosine phenolic ring in the *cis*-configuration (Figure 2D) relative to the $C\alpha{=}C\beta$ bond between the two cycles (Wall et al., 2000; Yarbrough et al., 2001). According to crystallographic data and high-resolution mass spectrometry, most anthozoan chromoproteins contain a DsRed-like chromophore including an acylimine substituent (Chan et al., 2006; Martynov et al., 2003; Pakhomov et al., 2006; Prescott et al., 2003). However, unlike DsRed, crystal structures of all known nonfluorescent GFP-like chromoproteins revealed a *trans*-noncoplanar chromophore configuration (Chan et al., 2006; Prescott et al., 2003). On the other hand, the far-red fluorescent protein eqFP611 from the sea anemone *Entacmaea quadricolor* bears the *trans*-coplanar chromophore (Petersen et al., 2003). Therefore, there is rather a correlation between the fluorescence quantum yield and chromophore planarity (Shu et al., 2006). Changes in planarity are associated with deviations of the two torsion angles (tilt and twist; Figure 2E) from 180°.

The *cis-trans* isomerism of the chromophore was proposed to be responsible for the photoactivatability phenomenon of the nonfluorescent anthozoan chromoproteins (asFP595, KFP) (Lukyanov et al., 2005). Nonfluorescent GFP-like chromoproteins can be transiently activated to a fluorescent state by illumination with light of an appropriate wavelength (Andresen et al., 2005; Chudakov et al., 2003; Henderson and Remington, 2006; Loos et al., 2006). Thus, the *cis-trans* isomerization of the chromophore appears to be a fundamental mechanism that is common to all reversibly photobleachable, photoswitchable, and photoactivatable GFP-like proteins (Henderson et al., 2007). However, it also appears that isomerization is solely a switch that controls some additional mechanisms which directly affect the protein fluorescence quantum yield. There are at least two possible scenarios for photoactivation of GFP-like proteins. First, photoactivation can be explained by the protein matrix-induced fixed planar conformation of the *cis*-isomer, which suppresses chromophore exocyclic torsional deformations and prevents nonradiative relaxation to the ground state. In contrast,

the nonplanar *trans*-isomer is partially disordered, probably because the chromophore pocket shape does not enable stabilization of any single configuration, which in turn favors conformational flexibility and lower quantum yields. Alternatively, the phenolic ring upon *trans-cis* photoisomerization may be oriented in such a way that there are few hydrogen-bond partners to stabilize the phenolate anion and, similarly to Dronpa, protonation/deprotonation equilibrium upon photoactivation may be shifted toward the protonated state (Henderson et al., 2007). Aside from photo-induced activation, all known chromoproteins can be converted to fluorescent analogs by point mutations (Bulina et al., 2002; Gurskaya et al., 2001). It is noteworthy that *trans-cis* isomerization can also be initiated by altering the pH, providing a model for exploring the mechanism of photoactivation (Battad et al., 2007).

Extension of GFP-like proteins into the far-red range (emission 610–650 nm) offers the possibility of suppressing light scattering and absorption by tissues which would result in better light penetration into live animal tissues. Imaging with far-red and near-infrared probes will provide a unique opportunity for noninvasive labeling and tracking of gene expression, tumor growth, and angiogenesis at the whole-body scale. Several far-red fluorescent proteins whose emission maxima reach the 650 nm wavelength have been developed thus far (Gurskaya et al., 2001; Shkrob et al., 2005; Wang et al., 2004). Recently, a bright far-red protein Katushka (λ_{em} = 635 nm) and its monomeric version mKate have been generated by site-specific and random mutagenesis of the protein eqFP578 from *E. quadricolor* (Shcherbo et al., 2007). More recently, far-red-shifted (λ_{em} = 639 nm) and folding-optimized variants of the fluorescent protein eqFP611 have been developed. An additional red shift of eqFP611 is proposed to be due to mutations that lead to a *trans-cis* isomerization of the chromophore. Thus, eqFP611 is the first example of GFP-like proteins in which both *cis* and *trans* isomers are brightly fluorescent (Kredel et al., 2008).

Probably, development of proteins with emission beyond 650 nm will require additional posttranslational modifications to further extend the conjugated π-electron system of the DsRed-like chromophore and to shift the protein absorbance to longer wavelengths. Alternatively, amino acid substitutions around the DsRed-like chromophore can result in proteins with larger Stokes shifts. Some low molecular weight dyes change their emission maximum with increasing solvent polarity due to the difference in dipole moment between the ground and excited states of the chromophore. Synthetic GFP chromophores exhibit this solvatochromic effect, substantially shifting their emission maxima as a function of solvent polarity (Dong et al., 2006). However, unlike synthetic chromophores, most GFP-like proteins show smaller Stokes shifts, and this has been attributed to the rigidity in the chromophore's environment necessary to exclude nonfluorescent relaxation to the ground state. By iterative somatic hypermutation and fluorescence-activated cell sorting, Wang et al. (2004) generated monomeric DsRed variants with increased photostability and far-red emission. By time-resolved fluorescence, Abbyad et al. (2007) compared the dynamic Stokes shifts of mPlum, the most red-shifted DsRed variant, and its evolutionary ancestors. The far-red emission of mPlum was attributed to a picosecond solvation response that was observed at all temperatures above the glass transition. This solvation response and a substantial dynamic Stokes shift of mPlum are possible if the region of the protein solvating the chromophore is capable of some flexibility. In contrast, evolutionary ancestors of mPlum did not show any time-dependent shift in emission. The changes in dipole moment between the ground and excited states of monomeric DsRed and mPlum were determined to be similar. Thus, the difference in Stokes shifts was proposed to be due to a single residue in close proximity to the mPlum chromophore, which is responsible for the solvation response (Abbyad et al., 2007). Optical properties of some wild-type and mutant proteins of the GFP family are summarized in Figure 3. The difference in slope of the lines connecting the absorbance and fluorescence scales at the left is due to variable Stokes shifts inherent to GFP-like proteins.

Crystallographic and mass spectrometric studies of a protein from *Zoanthus* sp. 2 suggested that, in contrast to DsRed, the red fluorescence of z2FP574 (red fluorescent protein from *Zoanthus* sp. 2) arises from a coupled oxidation-decarboxylation of Asp66, the first amino acid of the chromophore precursor DYG sequence (Pakhomov and Martynov, 2007; Pletneva et al., 2007a). Consequently, although the terminal acylimine-substituted *p*-HBI chromophore of z2FP574 is equivalent to that of DsRed, it appears to be the result of different posttranslational chemistry (Figure 1B). Furthermore, in contrast to DsRed, maturation kinetics of the wild-type and mutant proteins from *Zoanthus* species suggest that the anionic "green" GFP-like form is the actual intermediate producing the red species (Pakhomov and Martynov, 2007).

Subfamily of DsRed-Related Proteins

The reactive acylimine group of a DsRed-like chromophore is a potential source of additional posttranslational chemistry. One can observe acylimine reactivity upon protein denaturation, when H_2O addition across the acylimine C=N bond interrupts the extra conjugation of a DsRed-like chromophore and reverts its red-shifted spectra back to a GFP-like absorbance (Gross et al., 2000). However, compared with simple acylimines, the DsRed-like chromophore is less hydrolytically labile (Pakhomov et al., 2006; Turcic et al., 2006), probably due to the highly unsaturated *p*-HBI substituent. Autocatalytic posttranslational reactions at the acylimine yield a set of proteins, derivatives of DsRed (zFP538, mOrange, asFP595). However, neither the protein scaffold that controls acylimine reactivity nor the acylimine intermediate in the course of protein maturation have been identified directly. In contrast to the DsRed subfamily, additional posttranslational reactions within the DsRed-related proteins do not cause further extension of the chromophore π-system, which is reflected in tuning the emission range between 538 and 595 nm (Figure 3).

Posttranslational reactions at the acylimine were proposed to be responsible for the yellow fluorescence of the zFP538 protein from the button polyp *Zoanthus* sp. Crystal structures and mass spectrometric studies suggested that zFP538 contains a three-ring chromophore derived from a transimination reaction, in which the α-carbon of a proposed acylimine intermediate is attacked by the terminal amino group of chromophore-forming lysine 66 (Figure 1B, structure **VI**) (Pletneva et al., 2007b; Remington et al., 2005). The less effective charge delocalization in a cyclic imine, as compared with the acylimine substituent,

explains the hypsochromic shift of zFP538 (Remington et al., 2005). Another example of a blue shift arising from additional covalent modification of a DsRed-like chromophore is mOrange, the protein evolved from a monomeric DsRed variant (Shaner et al., 2004). mOrange undergoes a cyclization reaction, in which the hydroxy group of chromophore-forming threonine 66 apparently attacks the acylimine carbonyl carbon to form an unusual oxazole heterocycle (Figure 1B, structure **VIII**) (Shu et al., 2006).

Photoactivatable protein asFP595 from *Anemonia sulcata*, also termed kindling fluorescent protein (KFP), has extremely weak fluorescence at 595 nm (Lukyanov et al., 2000). However, upon illumination with green light, the protein is activated into a transiently fluorescent state that slowly relaxes back to the initial nonfluorescent state and can be quenched rapidly by illumination with blue light (Chudakov et al., 2003; Henderson and Remington, 2006). As discussed above, photoactivation of asFP595 is due to a *trans-cis* isomerism, which, similarly to Dronpa, can shift the protonation equilibrium toward the neutral protonated form. However, in contrast to Dronpa, the resting state of the asFP595 chromophore is *trans* nonfluorescent. Indeed, upon asFP595 activation, the absorbance peak at 568 nm, characteristic of the anionic chromophore, decreases considerably with a concomitant absorbance increase at 445 nm, suggesting that a protonation equilibrium is shifted toward the neutral form. Illumination at the absorbance maximum of the protonated asFP595 chromophore (~450 nm) accelerates recovery to the nonfluorescent resting state (Chudakov et al., 2003). Computational modeling of asFP595 absorbance spectra with quantum-chemical methods suggested that *trans*-to-*cis* isomerization is accompanied by protonation state changes and that the absorbing species populated upon photoactivation is the neutral *cis*-chromophore. In addition to the anionic and neutral forms, it has been proposed that a zwitterionic form may also exist. Hence a shift of the protonation equilibrium might also occur at the imine nitrogen of the imidazolinone ring (Schafer et al., 2007). However, the excitation maximum of photoactivated asFP595 is very close to the absorbance maximum before photoactivation. Moreover, the 445 nm-absorbing form of the activated protein was reported to be nonfluorescent. This argues in favor of the same chromophore charge of both initial nonfluorescent and activated asFP595, suggesting that some other mechanisms are responsible for asFP595 photoactivation (Chudakov et al., 2003).

Structural studies revealed that, unlike proteins of the DsRed subfamily, autocatalytic synthesis of the asFP595 chromophore is accompanied by a polypeptide chain break near the chromophore center (Quillin et al., 2005; Wilmann et al., 2005). The synthetic acetyl-substituted model chromophore in dimethylformamide exhibits absorbance and fluorescence spectra closely matching those of asFP595 (Yampolsky et al., 2005). Tandem mass spectral analysis of the terminal proteolytic peptides flanking the asFP595 chain break allowed the elucidation of the exact structure of the asFP595 chromophore (Figure 1B, structure **VII**), implying that the mature chromophore originates from a posttranslational hydrolysis reaction of an intermediate acylimine-substituted structure (Tretyakova et al., 2007).

Kaede Subfamily

Unlike the on-off fluorescence switching of photoactivatable proteins, photoconvertible fluorescent proteins are capable of being transformed from one emission maximum to another upon illumination at the appropriate wavelength. The Kaede (fluorescent protein from *Trachyphyllia geoffroyi*) subfamily represents the proteins that change their spectral properties irreversibly. They contain a chromophore derived from the tripeptide His-Tyr-Gly and initially emit green fluorescence. However, in contrast to oxidation of DsRed to the acylimine, Kaede-like proteins are driven into a red fluorescent state by irradiation with UV or violet light (Mizuno et al., 2003; Nienhaus et al., 2005; Pakhomov et al., 2004). The light-dependent conversion of these proteins is caused by polypeptide cleavage and generation of an additional double bond in the side chain of the histidine extending the conjugated system of a GFP-like chromophore by the histidine imidazole (Figure 1B, structure **V**). A protonated neutral form of a *p*-HBI chromophore is apparently involved in photoconversion and the reaction was proposed to proceed via an E2-type β elimination, which requires the neighboring glutamate as the base accepting one of the two C β protons of His62 (Nienhaus et al., 2005). Recent crystallographic studies suggest that photoconversion is assisted by a water molecule which is located in the vicinity of the His62 imidazole ring in the green form (Hayashi et al., 2007).

Kaede forms a homotetramer even at low concentrations of 1 nM. Similarly to avGFP, the phenolic group of the Kaede chromophore has neutral and anionic protonation states in an equilibrium. Time-resolved fluorescence measurements of the photoconverted red Kaede demonstrated that excitation of the neutral form eventually leads to the anionic excited state with a time constant of 13 ps at pH 7.5. This process was attributed to the fluorescence resonance energy transfer (FRET) from the photoexcited neutral form to the ground-state anionic form that is located in an adjacent subunit of the tetramer. The time-resolved fluorescence data measured at lowered pH revealed that ESPT also occurs in red Kaede with a time constant of 300 ps. Hence, FRET and ESPT take place simultaneously as competing processes. However, the ESPT rate in red Kaede was significantly slower than that in avGFP, which is likely due to the different hydrogen-bond network around the chromophore (Hosoi et al., 2006).

A photoconvertible mutant of the GFP-like protein KikG from the coral *Favia favus* has been evolved by replacing the original chromophore-forming tripeptide with the His-Tyr-Gly sequence and by subsequent semirational mutagenesis of the amino acids surrounding the chromophore (Tsutsui et al., 2005). Mutagenesis studies implied that histidine 62 is required, but not sufficient, for the β elimination reaction. Introduction of an additional seven mutations around the chromophore transformed KikG into the photoconvertible protein KikGR. In addition to UV or violet light, KikGR can be photoconverted by two-photon excitation at 760 nm, enabling cell labeling with better spatial resolution in thick and highly scattering tissues.

Concluding Remarks and Future Perspectives

Since the first report on the cloning of fluorescent proteins from Anthozoa in 1999, significant progress has been made toward understanding the structure and posttranslational chemistry of GFP-like proteins. This knowledge enables directed engineering of variants with altered absorption and emission spectra by modifying the π-electron system of the chromophore or

manipulating its environment. Further structural and biochemical studies will provide additional insight into how the protein scaffold controls the optical tuning process. We anticipate that future achievements will allow engineering of more finely tuned spectral variants and the extension of the spectral range of GFP-like proteins. In particular, new and improved photoactivatable and photoconvertible proteins, and bright variants emitting in the near-infrared region, would be highly desirable.

ACKNOWLEDGMENTS

This work was supported by grants from the Molecular and Cell Biology Program RAS and from the Russian Foundation for Basic Research (06-04-48196).

REFERENCES

Abbyad, P., Childs, W., Shi, X., and Boxer, S.G. (2007). Dynamic Stokes shift in green fluorescent protein variants. Proc. Natl. Acad. Sci. USA *104*, 20189–20194.

Ai, H.W., Shaner, N.C., Cheng, Z., Tsien, R.Y., and Campbell, R.E. (2007). Exploration of new chromophore structures leads to the identification of improved blue fluorescent proteins. Biochemistry *46*, 5904–5910.

Ai, H.W., Olenych, S.G., Wong, P., Davidson, M.W., and Campbell, R.E. (2008). Hue-shifted monomeric variants of Clavularia cyan fluorescent protein: identification of the molecular determinants of color and applications in fluorescence imaging. BMC Biol. *6*, 13.

Ando, R., Mizuno, H., and Miyawaki, A. (2004). Regulated fast nucleocytoplasmic shuttling observed by reversible protein highlighting. Science *306*, 1370–1373.

Andresen, M., Wahl, M.C., Stiel, A.C., Grater, F., Schafer, L.V., Trowitzsch, S., Weber, G., Eggeling, C., Grubmuller, H., Hell, S.W., and Jakobs, S. (2005). Structure and mechanism of the reversible photoswitch of a fluorescent protein. Proc. Natl. Acad. Sci. USA *102*, 13070–13074.

Andresen, M., Stiel, A.C., Trowitzsch, S., Weber, G., Eggeling, C., Wahl, M.C., Hell, S.W., and Jakobs, S. (2007). Structural basis for reversible photoswitching in Dronpa. Proc. Natl. Acad. Sci. USA *104*, 13005–13009.

Barondeau, D.P., Putnam, C.D., Kassmann, C.J., Tainer, J.A., and Getzoff, E.D. (2003). Mechanism and energetics of green fluorescent protein chromophore synthesis revealed by trapped intermediate structures. Proc. Natl. Acad. Sci. USA *100*, 12111–12116.

Barondeau, D.P., Tainer, J.A., and Getzoff, E.D. (2006). Structural evidence for an enolate intermediate in GFP fluorophore biosynthesis. J. Am. Chem. Soc. *128*, 3166–3168.

Barondeau, D.P., Kassmann, C.J., Tainer, J.A., and Getzoff, E.D. (2007). The case of the missing ring: radical cleavage of a carbon-carbon bond and implications for GFP chromophore biosynthesis. J. Am. Chem. Soc. *129*, 3118–3126.

Battad, J.M., Wilmann, P.G., Olsen, S., Byres, E., Smith, S.C., Dove, S.G., Turcic, K.N., Devenish, R.J., Rossjohn, J., and Prescott, M. (2007). A structural basis for the pH-dependent increase in fluorescence efficiency of chromoproteins. J. Mol. Biol. *368*, 998–1010.

Brejc, K., Sixma, T.K., Kitts, P.A., Kain, S.R., Tsien, R.Y., Ormo, M., and Remington, S.J. (1997). Structural basis for dual excitation and photoisomerization of the *Aequorea victoria* green fluorescent protein. Proc. Natl. Acad. Sci. USA *94*, 2306–2311.

Bulina, M.E., Chudakov, D.M., Mudrik, N.N., and Lukyanov, K.A. (2002). Interconversion of Anthozoa GFP-like fluorescent and non-fluorescent proteins by mutagenesis. BMC Biochem. *3*, 7.

Chan, M.C., Karasawa, S., Mizuno, H., Bosanac, I., Ho, D., Prive, G.G., Miyawaki, A., and Ikura, M. (2006). Structural characterization of a blue chromoprotein and its yellow mutant from the sea anemone *Cnidopus japonicus*. J. Biol. Chem. *281*, 37813–37819.

Chen, K.Y., Cheng, Y.M., Lai, C.H., Hsu, C.C., Ho, M.L., Lee, G.H., and Chou, P.T. (2007). Ortho green fluorescence protein synthetic chromophore; excited-state intramolecular proton transfer via a seven-membered-ring hydrogen-bonding system. J. Am. Chem. Soc. *129*, 4534–4535.

Chudakov, D.M., Feofanov, A.V., Mudrik, N.N., Lukyanov, S., and Lukyanov, K.A. (2003). Chromophore environment provides clue to "kindling fluorescent protein" riddle. J. Biol. Chem. *278*, 7215–7219.

Dong, J., Solntsev, K.M., and Tolbert, L.M. (2006). Solvatochromism of the green fluorescence protein chromophore and its derivatives. J. Am. Chem. Soc. *128*, 12038–12039.

Dong, J., Solntsev, K.M., Poizat, O., and Tolbert, L.M. (2007). The meta-green fluorescent protein chromophore. J. Am. Chem. Soc. *129*, 10084–10085.

Fron, E., Flors, C., Schweitzer, G., Habuchi, S., Mizuno, H., Ando, R., Schryver, F.C., Miyawaki, A., and Hofkens, J. (2007). Ultrafast excited-state dynamics of the photoswitchable protein Dronpa. J. Am. Chem. Soc. *129*, 4870–4871.

Giepmans, B.N., Adams, S.R., Ellisman, M.H., and Tsien, R.Y. (2006). The fluorescent toolbox for assessing protein location and function. Science *312*, 217–224.

Gross, L.A., Baird, G.S., Hoffman, R.C., Baldridge, K.K., and Tsien, R.Y. (2000). The structure of the chromophore within DsRed, a red fluorescent protein from coral. Proc. Natl. Acad. Sci. USA *97*, 11990–11995.

Gurskaya, N.G., Fradkov, A.F., Terskikh, A., Matz, M.V., Labas, Y.A., Martynov, V.I., Yanushevich, Y.G., Lukyanov, K.A., and Lukyanov, S.A. (2001). GFP-like chromoproteins as a source of far-red fluorescent proteins. FEBS Lett. *507*, 16–20.

Gurskaya, N.G., Fradkov, A.F., Pounkova, N.I., Staroverov, D.B., Bulina, M.E., Yanushevich, Y.G., Labas, Y.A., Lukyanov, S., and Lukyanov, K.A. (2003). A colourless green fluorescent protein homologue from the non-fluorescent hydromedusa *Aequorea coerulescens* and its fluorescent mutants. Biochem. J. *373*, 403–408.

Habuchi, S., Ando, R., Dedecker, P., Verheijen, W., Mizuno, H., Miyawaki, A., and Hofkens, J. (2005). Reversible single-molecule photoswitching in the GFP-like fluorescent protein Dronpa. Proc. Natl. Acad. Sci. USA *102*, 9511–9516.

Habuchi, S., Dedecker, P., Hotta, J., Flors, C., Ando, R., Mizuno, H., Miyawaki, A., and Hofkens, J. (2006). Photo-induced protonation/deprotonation in the GFP-like fluorescent protein Dronpa: mechanism responsible for the reversible photoswitching. Photochem. Photobiol. Sci. *5*, 567–576.

Hayashi, I., Mizuno, H., Tong, K.I., Furuta, T., Tanaka, F., Yoshimura, M., Miyawaki, A., and Ikura, M. (2007). Crystallographic evidence for water-assisted photo-induced peptide cleavage in the stony coral fluorescent protein Kaede. J. Mol. Biol. *372*, 918–926.

Heim, R., Prasher, D.C., and Tsien, R.Y. (1994). Wavelength mutations and posttranslational autoxidation of green fluorescent protein. Proc. Natl. Acad. Sci. USA *91*, 12501–12504.

Heim, R., Cubitt, A.B., and Tsien, R.Y. (1995). Improved green fluorescence. Nature *373*, 663–664.

Henderson, J.N., and Remington, S.J. (2005). Crystal structures and mutational analysis of amFP486, a cyan fluorescent protein from *Anemonia majano*. Proc. Natl. Acad. Sci. USA *102*, 12712–12717.

Henderson, J.N., and Remington, S.J. (2006). The kindling fluorescent protein: a transient photoswitchable marker. Physiology (Bethesda) *21*, 162–170.

Henderson, J.N., Ai, H.W., Campbell, R.E., and Remington, S.J. (2007). Structural basis for reversible photobleaching of a green fluorescent protein homologue. Proc. Natl. Acad. Sci. USA *104*, 6672–6677.

Hosoi, H., Mizuno, H., Miyawaki, A., and Tahara, T. (2006). Competition between energy and proton transfer in ultrafast excited-state dynamics of an oligomeric fluorescent protein red Kaede. J. Phys. Chem. B *110*, 22853–22860.

Karasawa, S., Araki, T., Nagai, T., Mizuno, H., and Miyawaki, A. (2004). Cyan-emitting and orange-emitting fluorescent proteins as a donor/acceptor pair for fluorescence resonance energy transfer. Biochem. J. *381*, 307–312.

Kredel, S., Nienhaus, K., Oswald, F., Wolff, M., Ivanchenko, S., Cymer, F., Jeromin, A., Michel, F.J., Spindler, K.D., Heilker, R., et al. (2008). Optimized and

far-red-emitting variants of fluorescent protein eqFP611. Chem. Biol. *15*, 224–233.

Labas, Y.A., Gurskaya, N.G., Yanushevich, Y.G., Fradkov, A.F., Lukyanov, K.A., Lukyanov, S.A., and Matz, M.V. (2002). Diversity and evolution of the green fluorescent protein family. Proc. Natl. Acad. Sci. USA *99*, 4256–4261.

Loos, D.C., Habuchi, S., Flors, C., Hotta, J., Wiedenmann, J., Nienhaus, G.U., and Hofkens, J. (2006). Photoconversion in the red fluorescent protein from the sea anemone *Entacmaea quadricolor*: is *cis-trans* isomerization involved? J. Am. Chem. Soc. *128*, 6270–6271.

Lukyanov, K.A., Fradkov, A.F., Gurskaya, N.G., Matz, M.V., Labas, Y.A., Savitsky, A.P., Markelov, M.L., Zaraisky, A.G., Zhao, X., Fang, Y., et al. (2000). Natural animal coloration can be determined by a nonfluorescent green fluorescent protein homolog. J. Biol. Chem. *275*, 25879–25882.

Lukyanov, K.A., Chudakov, D.M., Lukyanov, S., and Verkhusha, V.V. (2005). Innovation: photoactivatable fluorescent proteins. Nat. Rev. Mol. Cell Biol. *6*, 885–891.

Malo, G.D., Wang, M., Wu, D., Stelling, A.L., Tonge, P.J., and Wachter, R.M. (2008). Crystal structure and Raman studies of dsFP483, a cyan fluorescent protein from *Discosoma striata*. J. Mol. Biol. *378*, 869–884.

Martynov, V.I., Maksimov, B.I., Martynova, N.Y., Pakhomov, A.A., Gurskaya, N.G., and Lukyanov, S.A. (2003). A purple-blue chromoprotein from *Goniopora tenuidens* belongs to the DsRed subfamily of GFP-like proteins. J. Biol. Chem. *278*, 46288–46292.

Matz, M.V., Fradkov, A.F., Labas, Y.A., Savitsky, A.P., Zaraisky, A.G., Markelov, M.L., and Lukyanov, S.A. (1999). Fluorescent proteins from nonbioluminescent Anthozoa species. Nat. Biotechnol. *17*, 969–973.

Mena, M.A., Treynor, T.P., Mayo, S.L., and Daugherty, P.S. (2006). Blue fluorescent proteins with enhanced brightness and photostability from a structurally targeted library. Nat. Biotechnol. *24*, 1569–1571.

Mishin, A.S., Subach, F.V., Yampolsky, I.V., King, W., Lukyanov, K.A., and Verkhusha, V.V. (2008). The first mutant of the *Aequorea victoria* green fluorescent protein that forms a red chromophore. Biochemistry *47*, 4666–4673.

Mizuno, H., Mal, T.K., Tong, K.I., Ando, R., Furuta, T., Ikura, M., and Miyawaki, A. (2003). Photo-induced peptide cleavage in the green-to-red conversion of a fluorescent protein. Mol. Cell *12*, 1051–1058.

Mizuno, H., Mal, T.K., Walchli, M., Kikuchi, A., Fukano, T., Ando, R., Jeyakanthan, J., Taka, J., Shiro, Y., Ikura, M., and Miyawaki, A. (2008). Light-dependent regulation of structural flexibility in a photochromic fluorescent protein. Proc. Natl. Acad. Sci. USA *105*, 9927–9932.

Nguyen, A.W., and Daugherty, P.S. (2005). Evolutionary optimization of fluorescent proteins for intracellular FRET. Nat. Biotechnol. *23*, 355–360.

Nienhaus, K., Nienhaus, G.U., Wiedenmann, J., and Nar, H. (2005). Structural basis for photo-induced protein cleavage and green-to-red conversion of fluorescent protein EosFP. Proc. Natl. Acad. Sci. USA *102*, 9156–9159.

Nienhaus, K., Renzi, F., Vallone, B., Wiedenmann, J., and Nienhaus, G.U. (2006). Chromophore-protein interactions in the anthozoan green fluorescent protein asFP499. Biophys. J. *91*, 4210–4220.

Ormo, M., Cubitt, A.B., Kallio, K., Gross, L.A., Tsien, R.Y., and Remington, S.J. (1996). Crystal structure of the *Aequorea victoria* green fluorescent protein. Science *273*, 1392–1395.

Pakhomov, A.A., and Martynov, V.I. (2007). Chromophore aspartate oxidation-decarboxylation in the green-to-red conversion of a fluorescent protein from Zoanthus sp. 2. Biochemistry *46*, 11528–11535.

Pakhomov, A.A., Martynova, N.Y., Gurskaya, N.G., Balashova, T.A., and Martynov, V.I. (2004). Photoconversion of the chromophore of a fluorescent protein from Dendronephthya sp. Biochemistry (Mosc.) *69*, 901–908.

Pakhomov, A.A., Pletneva, N.V., Balashova, T.A., and Martynov, V.I. (2006). Structure and reactivity of the chromophore of a GFP-like chromoprotein from *Condylactis gigantea*. Biochemistry *45*, 7256–7264.

Palm, G.J., Zdanov, A., Gaitanaris, G.A., Stauber, R., Pavlakis, G.N., and Wlodawer, A. (1997). The structural basis for spectral variations in green fluorescent protein. Nat. Struct. Biol. *4*, 361–365.

Patterson, G.H., Knobel, S.M., Sharif, W.D., Kain, S.R., and Piston, D.W. (1997). Use of the green fluorescent protein and its mutants in quantitative fluorescence microscopy. Biophys. J. *73*, 2782–2790.

Patterson, G., Day, R.N., and Piston, D. (2001). Fluorescent protein spectra. J. Cell Sci. *114*, 837–838.

Petersen, J., Wilmann, P.G., Beddoe, T., Oakley, A.J., Devenish, R.J., Prescott, M., and Rossjohn, J. (2003). The 2.0-Å crystal structure of eqFP611, a far red fluorescent protein from the sea anemone *Entacmaea quadricolor*. J. Biol. Chem. *278*, 44626–44631.

Pletneva, N., Pletnev, V., Tikhonova, T., Pakhomov, A.A., Popov, V., Martynov, V.I., Wlodawer, A., Dauter, Z., and Pletnev, S. (2007a). Refined crystal structures of red and green fluorescent proteins from the button polyp Zoanthus. Acta Crystallogr. D Biol. Crystallogr. *63*, 1082–1093.

Pletneva, N.V., Pletnev, S.V., Chudakov, D.M., Tikhonova, T.V., Popov, V.O., Martynov, V.I., Wlodawer, A., Dauter, Z., and Pletnev, V.Z. (2007b). Three-dimensional structure of yellow fluorescent protein zYFP538 from Zoanthus sp. at the resolution 1.8 angstrom. Bioorg. Khim. *33*, 390–398.

Prescott, M., Ling, M., Beddoe, T., Oakley, A.J., Dove, S., Hoegh-Guldberg, O., Devenish, R.J., and Rossjohn, J. (2003). The 2.2 Å crystal structure of a pocilloporin pigment reveals a nonplanar chromophore conformation. Structure *11*, 275–284.

Quillin, M.L., Anstrom, D.M., Shu, X., O'Leary, S., Kallio, K., Chudakov, D.M., and Remington, S.J. (2005). Kindling fluorescent protein from *Anemonia sulcata*: dark-state structure at 1.38 Å resolution. Biochemistry *44*, 5774–5787.

Remington, S.J. (2006). Fluorescent proteins: maturation, photochemistry and photophysics. Curr. Opin. Struct. Biol. *16*, 714–721.

Remington, S.J., Wachter, R.M., Yarbrough, D.K., Branchaud, B., Anderson, D.C., Kallio, K., and Lukyanov, K.A. (2005). zFP538, a yellow-fluorescent protein from Zoanthus, contains a novel three-ring chromophore. Biochemistry *44*, 202–212.

Rizzo, M.A., Springer, G.H., Granada, B., and Piston, D.W. (2004). An improved cyan fluorescent protein variant useful for FRET. Nat. Biotechnol. *22*, 445–449.

Rosenow, M.A., Patel, H.N., and Wachter, R.M. (2005). Oxidative chemistry in the GFP active site leads to covalent cross-linking of a modified leucine side chain with a histidine imidazole: implications for the mechanism of chromophore formation. Biochemistry *44*, 8303–8311.

Schafer, L.V., Groenhof, G., Klingen, A.R., Ullmann, G.M., Boggio-Pasqua, M., Robb, M.A., and Grubmuller, H. (2007). Photoswitching of the fluorescent protein asFP595: mechanism, proton pathways, and absorption spectra. Angew. Chem. Int. Ed. Engl. *46*, 530–536.

Shagin, D.A., Barsova, E.V., Yanushevich, Y.G., Fradkov, A.F., Lukyanov, K.A., Labas, Y.A., Semenova, T.N., Ugalde, J.A., Meyers, A., Nunez, J.M., et al. (2004). GFP-like proteins as ubiquitous metazoan superfamily: evolution of functional features and structural complexity. Mol. Biol. Evol. *21*, 841–850.

Shaner, N.C., Campbell, R.E., Steinbach, P.A., Giepmans, B.N., Palmer, A.E., and Tsien, R.Y. (2004). Improved monomeric red, orange and yellow fluorescent proteins derived from Discosoma sp. red fluorescent protein. Nat. Biotechnol. *22*, 1567–1572.

Shaner, N.C., Patterson, G.H., and Davidson, M.W. (2007). Advances in fluorescent protein technology. J. Cell Sci. *120*, 4247–4260.

Shcherbo, D., Merzlyak, E.M., Chepurnykh, T.V., Fradkov, A.F., Ermakova, G.V., Solovieva, E.A., Lukyanov, K.A., Bogdanova, E.A., Zaraisky, A.G., Lukyanov, S., and Chudakov, D.M. (2007). Bright far-red fluorescent protein for whole-body imaging. Nat. Methods *4*, 741–746.

Shi, X., Abbyad, P., Shu, X., Kallio, K., Kanchanawong, P., Childs, W., Remington, S.J., and Boxer, S.G. (2007). Ultrafast excited-state dynamics in the green fluorescent protein variant S65T/H148D. 2. Unusual photophysical properties. Biochemistry *46*, 12014–12025.

Shkrob, M.A., Yanushevich, Y.G., Chudakov, D.M., Gurskaya, N.G., Labas, Y.A., Poponov, S.Y., Mudrik, N.N., Lukyanov, S., and Lukyanov, K.A. (2005). Far-red fluorescent proteins evolved from a blue chromoprotein from *Actinia equina*. Biochem. J. *392*, 649–654.

Shu, X., Shaner, N.C., Yarbrough, C.A., Tsien, R.Y., and Remington, S.J. (2006). Novel chromophores and buried charges control color in mFruits. Biochemistry *45*, 9639–9647.

Shu, X., Kallio, K., Shi, X., Abbyad, P., Kanchanawong, P., Childs, W., Boxer, S.G., and Remington, S.J. (2007). Ultrafast excited-state dynamics in the green fluorescent protein variant S65T/H148D. 1. Mutagenesis and structural studies. Biochemistry *46*, 12005–12013.

Sniegowski, J.A., Lappe, J.W., Patel, H.N., Huffman, H.A., and Wachter, R.M. (2005). Base catalysis of chromophore formation in Arg96 and Glu222 variants of green fluorescent protein. J. Biol. Chem. *280*, 26248–26255.

Stoner-Ma, D., Jaye, A.A., Ronayne, K.L., Nappa, J., Meech, S.R., and Tonge, P.J. (2008). An alternate proton acceptor for excited-state proton transfer in green fluorescent protein: rewiring GFP. J. Am. Chem. Soc. *130*, 1227–1235.

Tretyakova, Y.A., Pakhomov, A.A., and Martynov, V.I. (2007). Chromophore structure of the kindling fluorescent protein asFP595 from *Anemonia sulcata*. J. Am. Chem. Soc. *129*, 7748–7749.

Tsutsui, H., Karasawa, S., Shimizu, H., Nukina, N., and Miyawaki, A. (2005). Semi-rational engineering of a coral fluorescent protein into an efficient high-lighter. EMBO Rep. *6*, 233–238.

Turcic, K., Pettikiriarachchi, A., Battad, J., Wilmann, P.G., Rossjohn, J., Dove, S.G., Devenish, R.J., and Prescott, M. (2006). Amino acid substitutions around the chromophore of the chromoprotein Rtms5 influence polypeptide cleavage. Biochem. Biophys. Res. Commun. *340*, 1139–1143.

Verkhusha, V.V., Chudakov, D.M., Gurskaya, N.G., Lukyanov, S., and Lukyanov, K.A. (2004). Common pathway for the red chromophore formation in fluorescent proteins and chromoproteins. Chem. Biol. *11*, 845–854.

Wachter, R.M. (2007). Chromogenic cross-link formation in green fluorescent protein. Acc. Chem. Res. *40*, 120–127.

Wachter, R.M., King, B.A., Heim, R., Kallio, K., Tsien, R.Y., Boxer, S.G., and Remington, S.J. (1997). Crystal structure and photodynamic behavior of the blue emission variant Y66H/Y145F of green fluorescent protein. Biochemistry *36*, 9759–9765.

Wachter, R.M., Elsliger, M.A., Kallio, K., Hanson, G.T., and Remington, S.J. (1998). Structural basis of spectral shifts in the yellow-emission variants of green fluorescent protein. Structure *6*, 1267–1277.

Wall, M.A., Socolich, M., and Ranganathan, R. (2000). The structural basis for red fluorescence in the tetrameric GFP homolog DsRed. Nat. Struct. Biol. *7*, 1133–1138.

Wang, L., Jackson, W.C., Steinbach, P.A., and Tsien, R.Y. (2004). Evolution of new nonantibody proteins via iterative somatic hypermutation. Proc. Natl. Acad. Sci. USA *101*, 16745–16749.

Wilmann, P.G., Petersen, J., Devenish, R.J., Prescott, M., and Rossjohn, J. (2005). Variations on the GFP chromophore: a polypeptide fragmentation within the chromophore revealed in the 2.1-Å crystal structure of a nonfluorescent chromoprotein from *Anemonia sulcata*. J. Biol. Chem. *280*, 2401–2404.

Wilmann, P.G., Turcic, K., Battad, J.M., Wilce, M.C., Devenish, R.J., Prescott, M., and Rossjohn, J. (2006). The 1.7 Å crystal structure of Dronpa: a photo-switchable green fluorescent protein. J. Mol. Biol. *364*, 213–224.

Wood, T.I., Barondeau, D.P., Hitomi, C., Kassmann, C.J., Tainer, J.A., and Getzoff, E.D. (2005). Defining the role of arginine 96 in green fluorescent protein fluorophore biosynthesis. Biochemistry *44*, 16211–16220.

Wu, L., and Burgess, K. (2008). Syntheses of highly fluorescent GFP-chromophore analogues. J. Am. Chem. Soc. *130*, 4089–4096.

Yampolsky, I.V., Remington, S.J., Martynov, V.I., Potapov, V.K., Lukyanov, S., and Lukyanov, K.A. (2005). Synthesis and properties of the chromophore of the asFP595 chromoprotein from *Anemonia sulcata*. Biochemistry *44*, 5788–5793.

Yarbrough, D., Wachter, R.M., Kallio, K., Matz, M.V., and Remington, S.J. (2001). Refined crystal structure of DsRed, a red fluorescent protein from coral, at 2.0-Å resolution. Proc. Natl. Acad. Sci. USA *98*, 462–467.

